State Space Reconstruction Parameters in the Analysis of Chaotic Time Series - the Role of the Time Window Length

D. Kugiumtzis

Department of Informatics, University of Oslo,
P.O.Box 1080 Blindern, N-0316 Oslo, Norway

Abstract

The most common state space reconstruction method in the analysis of chaotic time series is the Method of Delays (MOD). Many techniques have been suggested to estimate the parameters of MOD, i.e. the time delay τ and the embedding dimension m. We discuss the applicability of these techniques with a critical view as to their validity, and point out the necessity of determining the overall time window length, τ_w, for successful embedding. Emphasis is put on the relation between τ_w and the dynamics of the underlying chaotic system, and we suggest to set $\tau_w \geq \tau_p$, the mean orbital period; τ_p is approximated from the oscillations of the time series. The procedure is assessed using the correlation dimension for both synthetic and real data. For clean synthetic data, values of τ_w larger than τ_p always give good results given enough data and thus τ_p can be considered as a lower limit ($\tau_w \geq \tau_p$). For noisy synthetic data and real data, an upper limit is reached for τ_w which approaches τ_p for increasing noise amplitude.

1 Introduction

State space reconstruction is the first step in non-linear time series analysis of data from chaotic systems including estimation of invariants and prediction. For a recent review of these topics see [1] and [2]. Reconstruction consists of viewing a time series $x_k = x(k\tau_s)$, $k = 1, \ldots, N$ in a Euclidean space $\mathbb{R}^m$, where m is the *embedding dimension* and τ_s is the sampling time. Doing this, we hope that the points in $\mathbb{R}^m$ form an attractor that preserves the topological properties of the original unknown attractor. A standard way to reconstruct the state space is the Method of Delays (MOD). Using MOD, each m-dimensional embedding vector is formed as $\mathbf{x}_k = [x_k, x_{k+\rho}, \ldots, x_{k+(m-1)\rho}]^T$ where ρ is a multiple integer of τ_s so that the *delay time* τ equals $\rho\tau_s$ [3]. The m coordinates of each point $\mathbf{x}_k$ are samples from the time series (separated by a fixed τ) covering a *time window* of length $\tau_w = (m-1)\tau$ (or $\tau_w = (m-1)\rho$ as multiple of τ_s).

The fundamental theorem of reconstruction, introduced first by Takens [4] [1] and extended more recently in [6], gives no restriction on τ while for m states the sufficient

---

[1] Similar work was made independently in [5].

1

(but not necessary) condition $m \geq 2d + 1$, where d is the fractal dimension of the underlying attractor [2]. Takens' theorem is valid for the case of infinitely many noise-free data. In practice, however, with a limited number of possibly noisy observations, the selection of τ and m is rather important for the quality of the reconstruction. Many methods have been suggested for estimating these parameters, but they are all empirical in nature and do not – as we show – necessarily provide appropriate estimates. This is a rather typical situation regarding state space reconstruction in general.

While there will always be uncertainties related to reconstruction from real data, it is still important to try to improve the procedures. We suggest τ_w as an independent parameter instead of focusing on the interrelated parameters τ and m of MOD. The time window length is of particular importance since it determines, in a certain sense, the amount of information passed from the time series to the embedding vectors. For a given τ_w, one may then select a sufficiently large m. Suggestions for the selection of τ_w have been made in [7], [8], [9], [10], [11] and [12] but to our knowledge there has been little systematic work regarding this parameter. We give procedures for estimating τ_w from the signal. Only time series from continuous systems are treated. For discrete systems, one typically sets $\rho = 1$, reducing the number of parameters to one – the embedding dimension, since $\tau_w = m - 1$.

The quality of the reconstructions is assessed using the correlation dimension [13]. The resulting reconstructions may not be the most suitable for other purposes such as estimation of Lyapunov exponents and prediction. However, with improved reconstructions for dimension estimation it is likely that the technique will be valuable also in other cases.

In section 2, we discuss several of the methods suggested up to now for estimating τ and m in MOD and comment on the underlying ideas as well as on the validity of the results. In section 3, we establish the role of τ_w in reconstruction and give simple ways to estimate it. Finally, in section 4, the correlation dimension is used to assess the proposed procedure using noise-free and noise-corrupted synthetic data as well as real data.

2   Suggested methods for estimating the MOD-parameters

A very helpful approach in visualizing the reconstruction problem is to consider the reconstruction as an orthogonal projection from some high p-dimensional state space onto an m-dimensional subspace defined by the m coordinates of the reconstructed vectors. Defining the linear mapping $B : \mathbb{R}^p \longrightarrow \mathbb{R}^m$, from each p-dimensional vector $\mathbf{x}_k^p$ to an m-dimensional vector $\mathbf{x}_k^m$, we have $\mathbf{x}_k^m = B\mathbf{x}_k^p$, where the rows of the $m \times p$ matrix B are orthonormal. The p coordinates of $\mathbf{x}_k^p$ are actually all the samples in the time window τ_w and in the case of MOD, where $p - 1 = \tau_w = (m - 1)\rho$, the m coordinates of the projected subspace are every ρ'th sample starting with the first, i.e. each row of B has one 1 and $p - 1$ zeros. Obviously, one can find other m-dimensional subspaces using a smaller ρ (which may not cover the whole τ_w). Using $\rho = 1$ results in an unfavorable reconstruction if the time series is densely sampled because then the attractor lies on the diagonal in $\mathbb{R}^m$. (The successive samples differ very little from each other.) In such a projection we utilize only the m first samples of τ_w. Other projections may be considered such as the one employed in the Singular Spectrum Approach (SSA) [7]. This method yields first a transformation of the natural coordinate

---

[2] Actually, Takens' condition uses $\lceil d \rceil$ instead of d, the topological dimension, i.e. the lower integer greater than d. The use of d in the inequality has been established in [6] allowing lower values for m.

system to another orthogonal system, ranking the p new directions according to the variance they explain, followed by a projection onto the m first directions. The rows of the B matrix are then the first m eigenvectors of the $p \times p$ sample covariance matrix of the embedding vectors. The reconstruction viewed as a projection from the hyperspace determined by τ_w reveals the importance of this parameter. For MOD, the subspace is defined completely by the parameters τ (or ρ) and m and for SSA by p and m.

Certain statements supporting current methods for estimating τ and m have been widely accepted and almost adopted as axioms. We do not intend to question all the existing methodology on MOD state space reconstruction, but feel that a discussion is needed regarding the guidelines used to choose the parameters.

2.1   Comments on the selection of the delay time

Consider first τ and the two following widely accepted criteria:

1. The reconstructed attractor must be expanded from the diagonal (implying that τ should not be too small) but not too much so that it folds back (implying that τ should not be too large).

2. The components of the vector $\mathbf{x}_k$ must be uncorrelated.

Note the similarity of the two criteria: increasing τ expands the attractor from the diagonal and the components get less correlated; beyond some range of τ, folding may occur and the components again get correlated. These goals are intuitively reasonable for $m = 2$, while the generalization to a larger m is not always straightforward as we show below. Many methods based on geometric properties seek the τ that makes the attractor cover the largest region or expands it maximally from the diagonal [14], [12], [15]. However, the goal of stretching the attractor from the diagonal to get "good" reconstructions is based rather on empirical than theoretical grounds. In theory, a good reconstruction means near topological equivalence of the reconstructed attractor to the original one. One way to assess topological equivalence is to check whether stretching and folding are proportionally the same in the two attractors. In practice, this is done by checking whether the inter-distances of points remain proportionally the same in the two attractors or, alternatively, by checking whether nearby points on the original attractor remain relatively close on the reconstructed attractor. This last property is not always preserved when we expand the attractor from the diagonal, even for proper expansions according to the two above criteria. We show this for the Lorenz system [16] in Fig. 1. Fig. 1a shows that when τ is very small ($\tau = 0.01$) the reconstructed attractor lies almost on the diagonal and the points are generally getting closer than the corresponding points on the original attractor. One expects that this problem is resolved when we expand the attractor sufficiently ($\tau = 0.18$ which gives the minimum of the so-called mutual information – see below). But the opposite phenomenon is observed instead as shown in Fig. 1b, i.e. points that are close on the original attractor become more distant on the reconstructed attractor. Further, we show in Fig. 1c that the distances are more balanced for the reconstruction with a comparably small value of τ ($\tau = 0.09$) which is not apparent from the two above criteria. The point we want to infer from this remark is that there is not necessarily a meaningful answer to the question: Why should we seek the τ that gives sufficient expansion from the diagonal? Expansion *per se* does not guarantee a configuration of the reconstructed attractor closer to the original one.
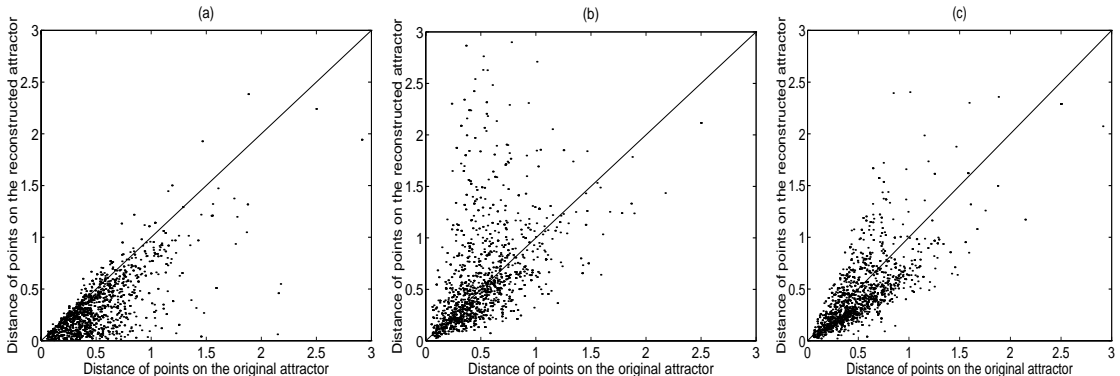
3

Figure 1: Correlation diagrams of the distances of points on the original attractor (x-axis) and on the reconstructed attractor (y-axis) for the Lorenz system. Results are shown for 10% of the 20000 data points sampled with $\tau_s = 0.01$ time units. For each point on the original attractor the distance from its nearest neighbor is computed and keeping track of the time indices the distance of the corresponding points on the reconstructed attractor is then found. The attractor is reconstructed with MOD, $m = 3$ and $\rho = 1$ in (a), $\rho = 18$ in (b), and $\rho = 9$ in (c).

Concerning the second criterion, the estimates for τ are based either on linear decorrelation, choosing τ such that $R(\tau) = 0$, where R is the autocorrelation function[3], or general decorrelation choosing τ to be the first minimum of the mutual information $I(\tau)$ as developed in [18]. These two methods guarantee decorrelation (linear or general) between two successive components x_k and $x_{k+\tau}$ of the reconstructed vector $\mathbf{x}_k$. But even if x_k and $x_{k+\tau}$ are uncorrelated and $x_{k+\tau}$ and $x_{k+2\tau}$ are uncorrelated, it does not follow that x_k and $x_{k+2\tau}$ are also uncorrelated. As an example, we show in Fig. 2 R and I for a time series from the Taylor-Couette experiment in the chaotic regime [19] which exhibits strong decorrelation for some lag τ and strong correlation for lag 2τ. We believe that the behavior of the correlation functions in Fig. 2 are often met in applications since chaotic time series from low dimensional systems frequently show pseudo-periodicities.

One may be confronted also with other problems attempting to estimate τ: the autocorrelation function may get approximately zero only after an extremely long time, as for the x-variable of the Lorenz system, or the mutual information may not have a clear minimum, as is the case with the physiological data used below.

2.2 Comments on the selection of the embedding dimension

The standard way to find m is to use some criterion which the geometry of the attractor must meet and check for which embedding dimension m^* this is fulfilled as the attractor is embedded in successively higher dimensional spaces. Then m^* is the lowest embedding dimension to be used for reconstruction. Obviously, in estimating m, τ is fixed when MOD is used.

Among different geometrical criteria (including also the correlation dimension), the most popular seems to be the method of "False Nearest Neighbors" (FNN) developed

---

[3]Other values of $R(\tau)$ such as $R(\tau) = 1/e$ have also been suggested but used little in applications, e.g. see [17].
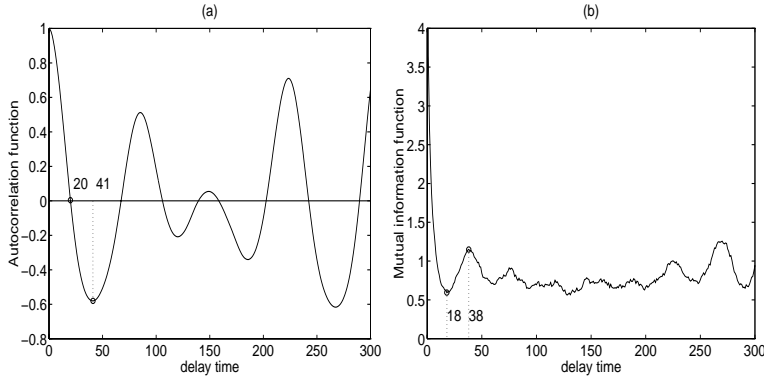
Figure 2: Autocorrelation function $R(\tau)$ in (a) and mutual information $I(\tau)$ in (b) for a time series of 10000 data measured from the Taylor-Couette experiment in the chaotic regime. Note the approximate matching of the zeros of R to minimums of I and the extremes of R to maximums of I indicating a dominant linear correlation. Moreover, note that the first decorrelation time is for $\rho \sim 20$ while for $\rho \sim 40$ there is maximum correlation.

in [20] and enhanced recently in [21]. The rationale behind this method has also been discussed in [22] and [23]. This criterion concerns the fundamental condition of no self-intersections of the reconstructed attractor. The original attractor lies on a smooth manifold of dimension $\lceil d \rceil$. Self-intersections of the reconstructed attractor indicate that it does not lie on a smooth manifold and thus the reconstruction is not successful. The condition of no self-intersections states that if the attractor is to be reconstructed successfully in $\mathbb{R}^m$, then all neighbor points in $\mathbb{R}^m$ should also be neighbors in $\mathbb{R}^{m+1}$. The method checks the neighbors in successively higher embedding dimensions until it finds only a negligible number of false neighbors when increasing the dimension from m^* to $m^* + 1$. This m^* is chosen as the lowest embedding dimension that gives reconstructions without self-intersections. However, the fact that the distances between neighboring points do not change when measured in $\mathbb{R}^m$ and in $\mathbb{R}^{m+1}$, does not necessarily mean that these points are also true neighbors on the original attractor.

Specifically, one has to consider the interdependence of m and τ. The estimation of m depends on the selection of τ (ρ) as we show in Fig. 3 for the Lorenz system. The proportion of false nearest neighbors does not fall to zero for the same m as τ increases but rather the estimated m increases slowly with τ. Thus, the estimation of m is somewhat arbitrary unless the method finds the same m for a sufficiently large range of τ values. For a very small τ, there is a typical underestimation of m. Such a τ forces the attractor to lie near the diagonal in $\mathbb{R}^m$. Increasing m by one has little effect on the geometry of the attractor as it will still lie near the diagonal of $\mathbb{R}^{m+1}$. All the points will apparently look as true neighbors leading to a wrong conclusion.

The method is very sensitive to noise giving larger values of m for noisy data as pointed in [23] and [24]. In fact, the effect of noise is greater for larger values of τ. This is a serious drawback of the method because in real applications we are led to choose a larger m than we really need. This problem is particularly relevant for MOD, where the projections are chosen without regard to noise filtering which is partly accomplished using SSA-reconstructions [9].

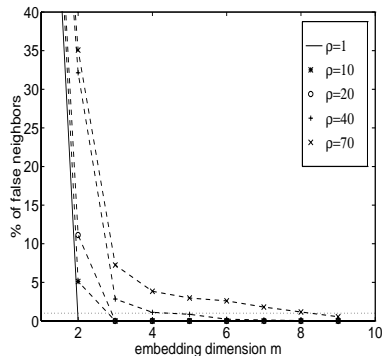Another method that has been suggested to estimate m is based on truncating the

5

Figure 3: Plot of the percent of false neighbors detected as the embedding dimension is increased for different values of τ. The algorithm of FNN has been implemented for a time series of 10000 samples of the x variable of the Lorenz system. The different curves correspond to the time delays given in the legend as multiple of the sampling time $\tau_s = 0.01$. The horizontal stippled line shows the 1% level of false neighbors which is often used as the discriminative threshold value.

singular spectrum of SSA (for details see [7] and [25]). In fact, the idea behind this linear approach is, given the hyperspace of dimension p, to find the smallest subspace (hyperplane) that approximately bounds the attractor. This subspace is spanned by the eigenvectors corresponding to the largest eigenvalues of the sample covariance matrix, i.e. the directions where the attractor has the largest variance. However, a strange attractor lies on a manifold which occupies all directions in the embedded space (very much like noise) and a clear cut-off is not expected [26]. On the other hand, if this approach is implemented locally it can reveal the dimension of the tangent space to the manifold and the averaging over a grid of local regions can give a robust estimate of m as shown in [27]. However, this estimate depends on the choice of the dimension p of the hyperspace, i.e. the time window length τ_w.

From these remarks we conclude that many of the existing methods for estimating τ and m are based on somewhat arbitrary criteria and do not always guarantee good reconstructions. The performance depends on the problem at hand.

3   The time window length - τ_w

When analysing a time series one typically begins with an initial reconstruction, and implements a non-linear method to this and other modified reconstructions until a stable result is attained. Here we concentrate on the time window length τ_w to determine the reconstruction.

There is probably no uniquely best way to choose an initial τ_w. We will argue that it may be reasonable to set τ_w equal to the "memory" of the system, i.e. the measurement record needed to determine future observations as reliably as possible. For practical reasons, one would like the shortest possible τ_w. Geometrically, one could associate such a τ_w with the *mean orbital period* τ_p, i.e. the mean time between two consecutive visits to a local neighborhood. For low-dimensional chaotic systems showing pseudo-periodicity, the mean orbital period could naturally be associated with the mean time between visiting a Poincare section.

6

For several chaotic systems, τ_p carries significant information about the dynamics. For systems that generate attractors with a sheet-like structure in $\mathbb{R}^3$ (see for example [28]), it can be shown that the Poincare section gives points that in a scatter plot lie approximately on a curve, which is the one dimensional manifold that embeds an attractor very much like the strange attractor of the logistic map. The same result may be obtained by selecting the points from the extremes or maxima of the time series directly instead of using reconstruction and Poincare section. This has been shown for the Lorenz system [29] and the Rössler system [30]. We found similar results studying the oscillations of other systems with sheet-like structure, such as the Rabinovich-Fabrikant system [31] and the Mackey Glass system for $\Delta = 17$ [32] (for details of this system see below).

As indicated above, the procedure suggested here requires only an initial estimate of τ_w which is subsequently adjusted. Given only a set of observations, a very simple solution is to select the initial τ_w as the mean *time between peaks* (*tbp*) of the original time series. In general, *tbp* will be less than τ_p, and thus it is natural to consider *tbp* a lower limit. For a low dimensional system, e.g. defined asymptotically in $\mathbb{R}^3$, it is reasonable to assume that an orbital period corresponds to an oscillation when projected down to the observed axis, and thus $\tau_p = tbp$. For more complicated systems in higher dimensional spaces, a complete orbit may form more than one oscillation. In that case, τ_p should be estimated as the average over a pattern of oscillations.

The equation of Mackey Glass [32]

$$\dot{x} = \frac{0.2x(t-\Delta)}{1 + [x(t-\Delta)]^{10}} + 0.1x(t) \tag{1}$$

is a good example to show how one can find lower limits for τ_w from the oscillations of the time series. This time delay differential equation was discretized following the iterative scheme in [33], and segments of the time series for different Δ are shown in Fig.4 with solid grey lines.
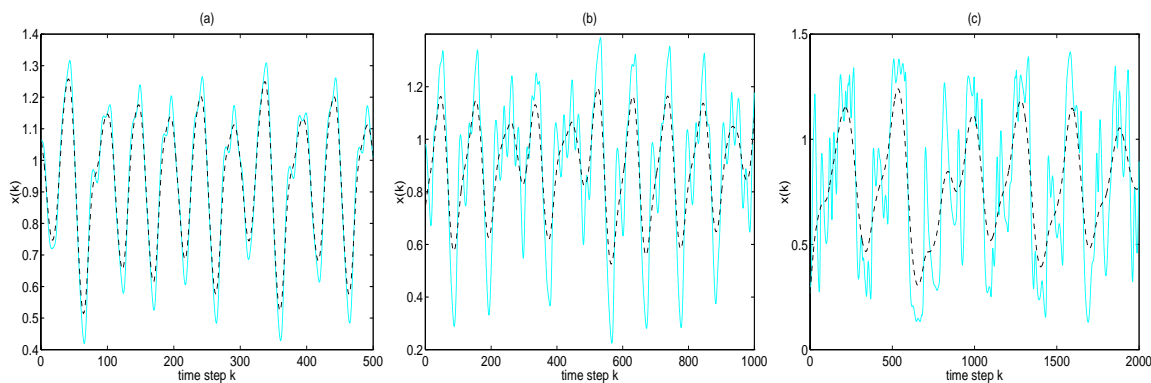

Figure 4: The solid grey lines in all three figures are for segments of the Mackey Glass time series for different Δ and the stippled lines after smoothing with a k-FIR filter. (a) $\Delta = 17$, $\tau_s = 1$, and $k = 10$. (b) $\Delta = 30$, $\tau_s = 1$, and $k = 30$. (c) $\Delta = 100$, $\tau_s = 1$, and $k = 80$.

For $\Delta = 17$, the attractor is low dimensional ($d \simeq 2$ [13]) and an orbital period can be assumed to correspond to a single oscillation (solid grey line in Fig. 4a). Then τ_p can be easily estimated as tbp after filtering the time series to avoid close peaks that

do not correspond to distinct oscillations (stippled black line in Fig. 4a), and thus for $\Delta = 17$ we can conclude that $\tau_w \geq \tau_p = tbp \simeq 50$ time units.

For $\Delta = 30$, the attractor has a higher dimension ($d \simeq 3$ [13]) and as Fig. 4b shows, in many parts of the time series there are systematic variations over a pattern of oscillations (often comprised of a small and a large oscillation), approximately repeating itself. Filtering gives a new time series with one peak for each such pattern, facilitating the computation of τ_p from the tbp of the filtered time series giving $\tau_w \geq \tau_p \simeq 100$.

For $\Delta = 100$ in Fig. 4c, the attractor is much more complicated ($d \simeq 7.1$ [33]) and therefore it is difficult to observe patterns of oscillations that repeat themselves (but not as difficult as to make Poincare sections). However, in some particular parts of the time series, consecutive similar patterns may be observed showing implicit correspondence to orbital periods (see Fig. 4c). Hard filtering allows us even to assign a peak to each pattern giving $\tau_w \geq \tau_p \simeq 330$. Note that filtering is performed only in order to discern the representative peaks, especially for higher dimensional systems. Noisy time series should be filtered anyway, before estimating τ_p to avoid the fake peaks that are due to noise.

Up to this point we have assumed that the measurement function is well defined according to Takens' generic assumptions, so that the oscillations in the observed time series do reflect the periodic-like orbits of the original system and vice versa. However, this is not always the case and as an example of a "good" and "bad" mapping let us consider the x and z variable of the Rössler system [34] (see Fig. 5). In the time series
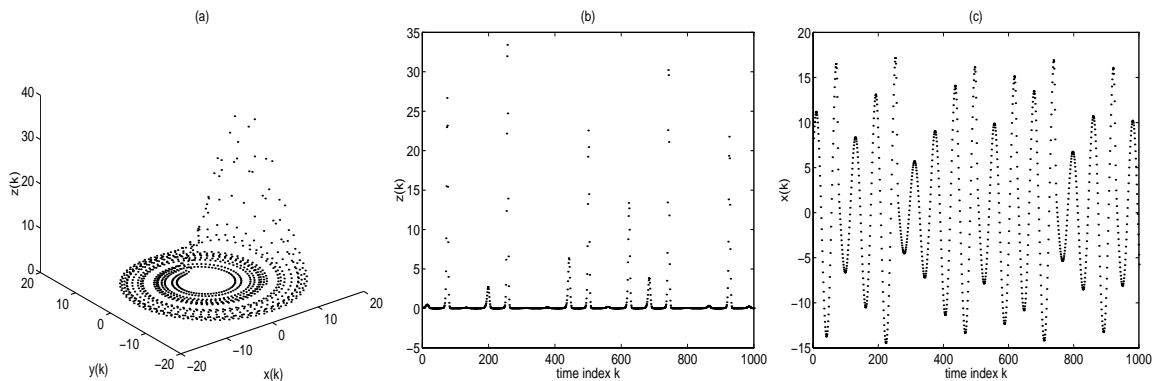

Figure 5: (a) A trajectory of the Rössler system in $\mathbb{R}^3$. (b) Measurements of the z variable of the trajectory. (c) Measurements of the x variable of the trajectory. Note that the oscillations of the time series in (b) do not reveal all orbital periods associated with the trajectory while in (c) they do.

of the x variable, the oscillations represent the real orbits while in the time series of the z variable the orbital periods can hardly be recognized. In the latter case, an analysis will fail to identify the correct attributes of the system unless a very large amount of data is provided to compensate for the bad mapping. We found, for example, that for measurements over the same epoch, the correlation dimension of the Rössler attractor was well estimated by the x-measurements but significantly underestimated by the z-measurements due to the "knee" phenomenon we discuss below.

We here suggest working directly in the time domain to estimate τ_w instead of considering periods corresponding to dominant frequencies as suggested by [7] and [10]. Chaotic data will in general not show well defined frequency peaks. Other suggestions

regarding τ_w have been presented in the literature [8], [11] and [12]. Some attempted to estimate τ_w based on decorrelation criteria from the autocorrelation function and the mutual information [9], [35] and [36]. In one paper treating this issue, [9], lower and upper limits for τ_w where based on the autocorrelation function and it was proposed to set $\tau_c \leq \tau_w \leq 4\tau_c$, where τ_c is the correlation time defined as the delay where the autocorrelation function is $1/e$. This lower limit is much smaller than τ_p for most systems. An upper limit for τ_w was given in [11] by $2\sqrt{\frac{3\langle x^{(0)}\rangle}{\langle x^{(1)}\rangle}}$, where $\langle x^{(0)}\rangle$ and $\langle x^{(1)}\rangle$ are the mean values of the time series and its first derivative, respectively. We found that for many systems this upper limit is also smaller than τ_p.

4 Correlation dimension and τ_w

We now discuss the use of τ_w in the time series analysis. A natural procedure is to start with an initial τ_w and perform calculations – in this case computing the correlation dimension ν – for a sufficiently large m. Then τ_w is modified, the calculations repeated, and so on. To be able to conclude that a valid result has been obtained, reasonably stable values have to be found over a range of τ_w values.

First we define the correlation integral $C(r)$, a statistic that measures the fraction of points on the attractor being less than r units apart

$$C(r) = \frac{1}{N(N-1)} \sum_{i,j=1,\,|i-j|>K}^{N} \Theta(r - ||\mathbf{x}_i - \mathbf{x}_j||) \tag{2}$$

where $\Theta(x)$ is the Heaviside function, defined as $\Theta(x) = 1$ for $x \geq 0$ and $\Theta(x) = 0$ for $x < 0$, and K is used to omit time-correlated points in the computation of $C(r)$. The Euclidean norm is used because it gives more robust results in the presence of noise [37]. For deterministic systems, the correlation integral scales as $C(r) \sim r^\nu$, where theoretically $r \to 0$. Preferably, ν should be estimated from the slope of the graph of $\log C(r)$ against $\log r$ over a sufficient range $[r_1, r_2]$ of small interdistances. However, due to noise or to limited data, an approximately constant slope may be maintained only for larger values of r_1 and r_2. We chose $r_2/r_1 = 4$ for the length of the interval, and searched over all such intervals to find the one where the computed ν varied least[4]. The mean value of the slope in this interval is the estimated ν, and it is always reported together with the standard deviation (shown with bars in the following figures).

A key observation is that the estimate of the correlation dimension of a chaotic time series (clean or noisy) is approximately the same under variations of the parameters ρ and m while keeping $\tau_w = (m-1)\rho$ fixed (assuming that m is always larger than the dimension of the attractor). Only few workers seem to have thought along these lines ([8], [9], [10] and [12]). The typical features are demonstrated in Fig. 6 which shows the correlation dimension estimates for different τ_w for clean and noisy data from the Lorenz system. Note how the grey and black curves match for the clean data in Fig. 6a. They correspond to the same τ_w but with $\rho = 2$ and $\rho = 10$, respectively. Once τ_w, and thus the p-dimensional hyperspace, has been determined, the particular projection chosen is not critical as long as the projection is sufficient, i.e. $m > \nu$ and $\rho \simeq \frac{p-1}{m-1} \equiv \frac{\tau_w}{m-1}$. This is so, because the interdistances of points remain statistically the same in $\mathbb{R}^p$ and in $\mathbb{R}^m$. Considering all the coordinates or only the selected subset

---

[4]To compute the slope for each r we use the best fit slope for three values, the current r, the previous and the next.
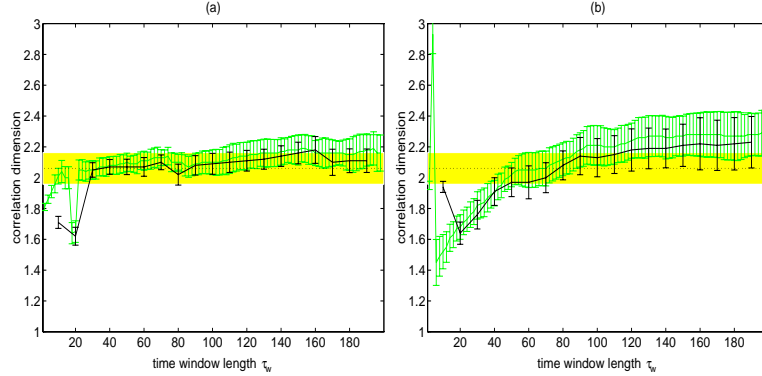
Figure 6: Plot of the correlation dimension estimate ν for MOD reconstruction with different τ_w for time series of the x variable of the Lorenz system. The bars denote the standard deviation of the estimate. In each figure the grey curve with grey error bars correspond to $\rho = 2$ while the black ones to $\rho = 10$. In (a) the estimation is based on the clean time series of 4000 data sampled with $\tau_s = 0.02$ and in (b) on the same data but corrupted with 5% noise. The horizontal stippled line shows the correct plateau for $\nu = 2.06$ and the shaded area the confidence interval of $\pm 5\%$ of the correct ν.

has the same effect on the computation of the interdistance as long as a suitable norm is used, e.g. the Euclidean norm [37].

When white noise is added to the clean Lorenz data (Fig. 6b) the two curves still match but now show an increasing trend with τ_w. The estimation of ν is more sensitive to the choice of τ_w in the presence of noise.

Results for the estimation of ν from noisy data or few data (compared to the minimum number of data required) should be interpreted with caution because they are derived from scaling properties based on large r. For smaller r, the scaling is corrupted by noise or distorted due to few neighbors in state space. In the case of attractors with different scaling properties for small and large r (a phenomenon referred to as a "knee" [38]), erronous estimates are obtained from the scaling for large r when noise or insufficient data length mask the correct scaling for small r. Such a phenomenon is observed for the z-measurements of the Rössler system mentioned before. The correct scaling ($\nu \simeq 2.01$) can be only detected for very small inter-point distances r requiring a very large number of data, otherwise another scaling is detected for larger r, underestimating ν.

The estimation of ν, even when it is constrained only to large r, is not straightforward as it varies with τ_w and a typical situation is shown in Fig. 7 for Lorenz system. Too small τ_w ($\tau_w = 20$) or too large τ_w ($\tau_w = 160$) gives uncertain and wrong estimates while for τ_w larger than but still close to $\tau_p = 50$ (here $\tau_w = 80$)[5] the scaling is clear indicating a reliable estimate. On the other hand, the range of suitable τ_w depends on the length of the time series; the longer the time series, the broader the limits for τ_w. Noise also restricts τ_w from above because the slope curves derived for increasing τ_w do not saturate. Setting a criterion for the acceptance of the ν-estimate, e.g. $\pm 5\%$ of the correct value, an upper limit τ_n for the range of τ_w may be found which varies with the amplitude of the noise (e.g. $\tau_n \simeq 110$ for Fig. 6b). It is thus expected that the

---

[5]For this time series the periods of the oscillations vary a lot and thus the estimate τ_p has large variance and does not completely indicate the "memory of the system".
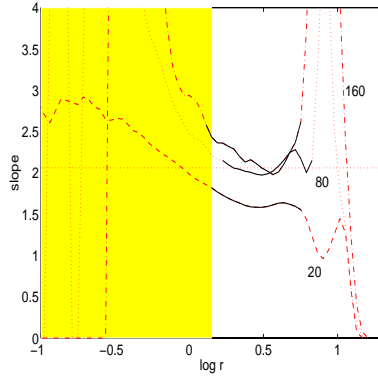
Figure 7: Plot of the slope of the graph $\log C(r)$ against $\log r$ for the time series of 4000 data from the Lorenz system, sampled with $\tau_s = 0.02$ and with 5% additive noise. The three curves are derived from reconstructions with $\rho = 10$ and $m = 3$ (minimum embedding dimension), $m = 9$ and $m = 17$ and are identified by the length of τ_w marked on the figure. The scaling interval of least variation is denoted with the black solid line segment for each slope curve. The grey area shows roughly the region where inter-point distances are corrupted by noise leaving a small interval of r to estimate ν and making the choice of τ_w critical. The horizontal stippled line shows the correct plateau for $\nu \simeq 2.06$.

scaling gets distorted as τ_w icreases over τ_n giving less confident estimates as shown with the slope curve for $\tau_w = 160$ in Fig. 7. So, when the time series is corrupted with noise, the ν-estimates are more biased and the interval $[\tau_p, \tau_n]$ of the accepted τ_w shrinks from above, and it may be no reliable estimate of ν for any τ_w if the impact of noise is so large that τ_n decreases to the level of τ_p.

Thus when estimating ν from a limited number of noisy data we seek the range of τ_w that gives clear scaling for large r keeping in mind that the results are still ambiguous due to the possible different scaling for small and inaccessible r (the "knee" phenomenon). In the sequel, we consider in more detail simulated data corrupted with noise as well as real data.

4.1 Noisy synthetic data

Most of the time series we use here have length $N = 4000$ adjusting the sampling time τ_s accordingly in order to have enough oscillations as well as enough samples for each oscillation. It follows that the number of data points is not the best measure of the record length. We therefore also quote the number of τ_p within the record, denoted $\#\tau_p$, together with the number of samples in τ_p. Note that under changes of the reconstruction parameters or the noise amplitudes, the values r_1 and r_2 of the scaling interval $[r_1, r_2]$ that gives ν-estimates with least variance may change as well.

Results for the time series from the x-variable of the Lorenz system with $\tau_s = 0.02$ and $\tau_p \simeq 50$ and $\#\tau_p \simeq 80$ were shown in Fig. 6. For the clean data, legitimate estimates of ν (within $\pm 5\%$ of the correct $\nu = 2.06$ shown as a shaded zone in the figure) were obtained for a large interval of τ_w values beginning even lower than τ_p. As τ_w is increased long beyond τ_p the estimates increase somewhat and have larger variance. When 5% white Gaussian noise is added to these data, the correlation dimension is

11

underestimated significantly for $\tau_w < \tau_p$, and for $\tau_w > \tau_n \simeq 110$, ν is overestimated with larger variance.

The attractor derived from the x-variable of the Rössler system has a simpler structure than the Lorenz attractor and about the same dimension. However, estimates of ν are more dependent on the reconstruction parameters and the amplitude of the noise. The time series is sampled with $\tau_s = 0.1$ that gives 60 samples in each oscillation and about 66 oscillations, which are comparable to the τ_p and $\#\tau_p$ for the Lorenz data. In Fig. 8, the ν-estimates are plotted against τ_w for the clean and noisy Rössler data
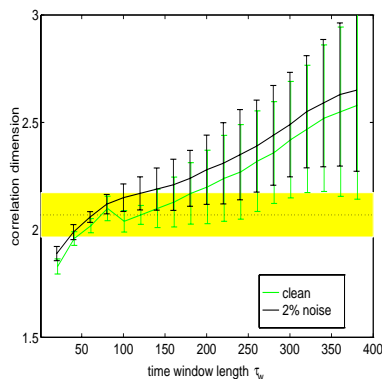

Figure 8: Plot of the correlation dimension estimate ν for MOD reconstruction with different τ_w for time series of the x variable of the Rössler system. The grey curve with grey error bars correspond to the clean data and the black to the same data corrupted with 2% noise. Here, $N = 4000$, $\tau_s = 0.1$ and $\rho = 20$. The horizontal stippled line shows the correct plateau for $\nu = 2.01$ and the shaded area the confidence interval of $\pm 5\%$ of the correct ν.

displayed with grey and black error bars respectively, together with the $\pm 5\%$-zone of the accepted range of ν. Here, as well as in the following estimations, we keep ρ fixed ($\rho = 20$ in Fig. 8) and vary m. This is done for convenience since the results are essentially the same for other combinations of ρ and m (refer back to Fig. 6). For the clean data, reasonable and confident ν-estimates can be found for a small range of $\tau_p = 60 \leq \tau_w < 140$ (the grey error bars in the $\pm 5\%$-zone in the figure). When just 2% white noise is added to these data, the small horizontal plateau seems to disappear (the black line in Fig. 8) and only ν-estimates close to τ_p and above can be accepted, which is in accordance with the proposed τ_w.

The Mackey Glass attractor for $\Delta = 17$ has the same dimensionality as the two last attractors but gives less biased estimates of ν. For $\tau_s = 1$, we found $\tau_p = 50$ and $\#\tau_p \simeq 80$ from single oscillations. In Fig. 9, results from the estimation of ν are presented in the same way as for the Rössler data. For the clean data, a very reliable ν-estimate is derived over a large interval of τ_w, $[20, 160]$ (from the $\pm 5\%$-criterion). When 5% noise is added, confident estimates are obtained only close to τ_p, and when 10% noise is added, reasonable estimates are only obtained for $\tau_w \simeq \tau_p$.

When $\Delta = 30$, the dimension of the attractor increases to $\nu \simeq 3$ [13]. However, using $N = 4000$ and $\tau_s = 2$ an underestimate ($\nu \simeq 2.5$) was found. For this τ_s, the τ_p estimated with the mean time for patterns of two oscillations (cf. section 3) is kept down to $\tau_p = 50$ and $\#\tau_p \simeq 80$, as for $\Delta = 17$. The results from estimation of ν for clean and noisy data with 5% and 10% noise (shown in Fig. 10a) assert the
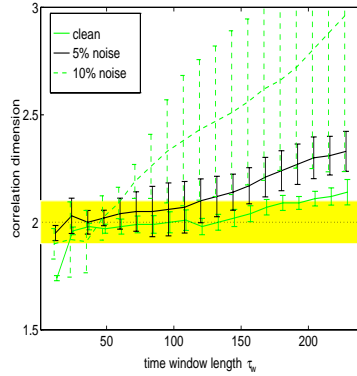
Figure 9: Plot of the correlation dimension estimate ν for MOD reconstruction with different τ_w for time series of the Mackey Glass equation for $\Delta = 17$. The solid grey curve with solid grey error bars correspond to the clean data, the solid black to the noisy data with 5% noise and the stippled grey to the noisy data with 10% noise. Here, $N = 4000$, $\tau_s = 1$ and $\rho = 12$. The horizontal stippled line shows the correct plateau for $\nu = 2$ and the shaded area the confidence interval of $\pm 5\%$ of the correct ν.

use of τ_p as a lower limit for τ_w and the decrease of the interval of accepted values for τ_w from above and towards τ_p as the amplitude of the added noise is increased. The underestimation of ν is due to the limited number of data. This attractor shows a "knee" structure, i.e. it has also another scaling (the correct $\nu \simeq 3.0$) for small r which can be detected only when many data are accumulated as shown in Fig. 10b. The slope for too small τ_w ($\tau_w = 24$) underestimates ν while for $\tau_w \geq \tau_p$ the correct scaling is achieved (shown with the two curves for $\tau_w = 48$ and $\tau_w = 168$ in the figure). Note that these curves form a second scaling for larger r.

For $\Delta = 100$, the Mackey Glass attractor gets high dimensional with $\nu \simeq 7$ [33]. Our results show a slightly lower ν with as few as $N = 4000$. We sampled the discretized system with $\tau_s = 10$ in order to have enough, but not too many, samples within the estimated mean orbital period, $\tau_p \simeq 33$, giving as many as $\#\tau_p \simeq 120$ repititions of the oscillation pattern that is assumed to correspond to an orbit of the underlying system. We deliberately keep the data record down to $N = 4000$ in order to test our procedure for short time series (compared to the high dimensionality of the system). The estimated ν is an increasing function of τ_w both in values and uncertainty, showing some stability in value and in variance for $\tau_p \simeq 30 \leq \tau_w \leq 45$. This is, however, an underestimation of ν, possibly due to insufficient data (see Fig. 11). Adding 5% noise does not alter the ν-estimates but just increases moderately the uncertainty of the estimates; when 10% noise is added, the ν-estimates for $\tau_w > \tau_p$ vary significantly from those of the clean data.

These findings, as well as results for the Rabinovich-Fabrikant system [31], and the four-dimensional Rössler Hyperchaos system [39], not shown here, confirm our suggestion for estimating τ_w with τ_p giving the best estimates of ν. If the effect of noise or limited length of the time series is such that estimation of ν can be made only for a short range of τ_w values, this is close to and little larger than τ_p.
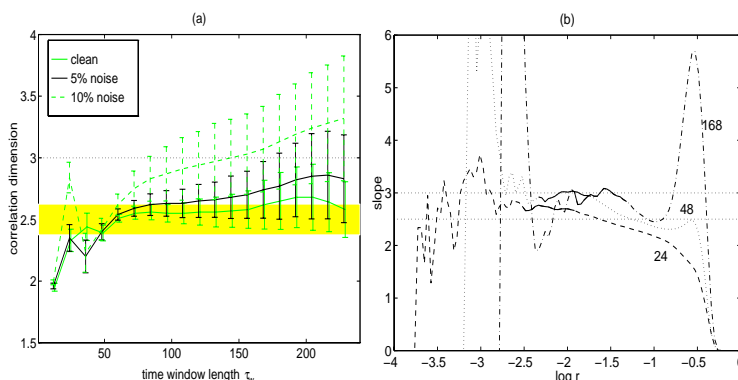
13

Figure 10: (a) Plot of the correlation dimension estimate ν for MOD reconstruction with different τ_w for time series of the Mackey Glass equation for $\Delta = 30$. The solid grey curve with solid grey error bars correspond to the clean data, the solid black to the noisy data with 5% noise and the stippled grey to the noisy data with 10% noise. Here, $N = 4000$, $\tau_s = 2$ and $\rho = 12$. The horizontal stippled line shows the correct plateau for $\nu \simeq 3.0$ and the shaded area the confidence interval of $\pm 5\%$ of the underestimated $\nu \simeq 2.5$. (b) Plot of the slope of the graph $\log C(r)$ against $\log r$ for the same type of data but for $N = 30000$. The three curves are derived from reconstructions with $\rho = 12$ and $m = 3$, $m = 6$ and $m = 17$ and are identified by the length of τ_w marked on the figure. The scaling interval of least variation is denoted with the black solid line segment for each slope curve. The two horizontal stippled lines show the two scalings of this attractor.

4.2   Real data

In addition to simulated data, observations from physical controlled experiments on low dimensional deterministic processes should be used to assess the validity of non-linear methods. The noise level is often insignificant in such cases. Here we use a time series of $N = 4000$ samples from the Taylor Couette experiment in the chaotic regime. We estimated $\tau_p \simeq 75$ and $\#\tau_p \simeq 54$, but the results for the estimation of ν do not change for longer time records covering more oscillations (increasing either N or τ_s if we insist on keeping N small). Contrary to most of the previous results from simulated data with noise, the estimated ν varies little with τ_w as shown in Fig. 12. For all $\tau_w > \tau_p$ the etsimates are more or less fixed to $\nu \simeq 2.6$, approximately the value given in the literature [19], with a slowly increasing uncertainty for $\tau_w > 150$. This indicates that there is little noise in the data and the dimension of the chaotic attractor can be identified even with large τ_w (up to $2\tau_p$), so that the choice of τ_w is not critical. However, when we add noise to these data, to simulate a larger experimental uncertainty, the estimates have as expected a larger variance, but for τ_w close to τ_p the estimates are the same as for the original time series. For larger τ_w there is a systematic overestimation of ν, showing again that the optimal τ_w for correct estimation is close to τ_p.

We now turn to observational data that are not output of a controlled experiment, and concentrate on physiological data of the Electroencephalogram (fig13) from epileptic patients (e.g. see [40]). Dimension estimation of physiological data has been a hot subject the last years. However, the results to date are not promising, partly because different procedures are often used giving different ν-estimates for the same type of
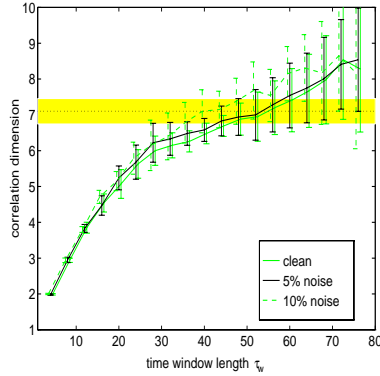
14

Figure 11: Plot of the correlation dimension estimate ν for MOD reconstruction with different τ_w for time series of the Mackey Glass equation for $\Delta = 100$. The solid grey curve with solid grey error bars correspond to the clean data, the solid black to the noisy data with 5% noise and the stippled grey to the noisy data with 10% noise. Here, $N = 4000$, $\tau_s = 10$ and $\rho = 4$. The horizontal stippled line shows the correct plateau for $\nu \simeq 7.1$ and the shaded area the confidence interval of $\pm 5\%$ of the correct ν.

data, and partly because these data do not seem to share the same nice chaotic properties as the well-studied simulated data [41]. Previous work on ν-estimation of EEG epileptic signals reported low dimensional attractors of varying dimension between 2 and 6, according to the physiological nature of the data, the data acquisition process, the computational scheme of estimation, as well as the parameter setting for reconstruction ([42], [43], [44] and [45]).

Here, we use a short time series from an epileptic seizure of $N = 3400$ data sampled with $\tau_s = 0.005 sec$. The oscillations of the time series evolve irregularly, so the estimated $tbp \simeq 30$ does not seem to be directly related to τ_p. With a more thorough examination of the sequence of oscillations, we can distinguish patterns of oscillations that may correspond to orbital periods of the potential underlying attractor. In Fig. 13a we show a part of the time series where such patterns are apparent. After severe filtering, the time corresponding to each pattern can be estimated by the tbp for the filtered time series giving $\tau_p \simeq 110$. Other parts of the time series are not so regular but still patterns of about the same time length can be identified qualitatively. The standard estimation procedure applied to these data gave no clear saturation of the ν-estimate for increasing τ_w, (grey curve in Fig. 13b). The estimate increases with increasing variance showing some flatness for a small region of values of τ_w around 100. In fact, for $\tau_w > 100$ there is scaling but over a shorter interval of interdistances $[r1, r2]$ not satisfying the more stringent criterion $r2/r1 = 4$. Relaxing this to $r2/r1 = 2$, which has previously been used for EEG signals [46], a clear saturation with $\nu \simeq 4$ is established for $\tau_w > 100$, though with increasing variance (Fig. 13b). Thus, the optimal choice of τ_w for the computation of ν should be around 100, which is close to $\tau_p = 110$, the estimate of τ_w from the oscillations of the time series. Note that these results are not general for epileptic EEG signals. Other EEG data showed very poor scaling and no saturation for increasing τ_w even for $r2/r1 = 2$ [47] giving no valid estimate for ν. In these cases, no patterns of oscillations could be observed.
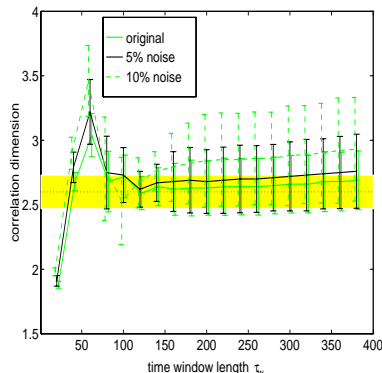
15

Figure 12: Plot of the correlation dimension estimate ν for MOD reconstruction with different τ_w for time series from the Taylor Couette experiment in the chaotic regime. The solid grey curve with solid grey error bars correspond to the original data, the solid black to the original data corrupted with 5% noise and the stippled grey to the original data corrupted with 10% noise. Here, $\rho = 20$ is chosen for reconstructions varying with m. The horizontal stippled line shows the correct plateau for $\nu \simeq 2.6$ and the shaded area the confidence interval of $\pm 5\%$ of the correct ν.

5 Conclusions

Our analysis in section 2 showed that when one reconstructs with MOD, effective techniques for determining the delay time τ and the lowest embedding dimension m are lacking. Concerning τ, there is no standard indication of which value is the most appropriate. In fact, if we allow m to be very large, we can even use a very small τ in the reconstruction. It seems that instead of relying on estimates for τ (such as the zero of the autocorrelation function or the minimum of mutual information) and m (such as the estimate from false nearest neighbors) one could rather employ "trial and error". In fact, this seems to be common in practice.

A more systematic and less tedious way to make reconstructions has been proposed here focusing on the time window length τ_w. We argued that τ_w is the first parameter to be determined when reconstructing the state space and suggested that it should be approximated by the mean orbital period τ_p. For low dimensional attractors, τ_p is set to the time between peaks tbp, easily calculated by averaging the time between successive maxima of the time series. Noisy time series may be filtered before determining tbp. For higher dimensional and more complicated systems, the mean orbital period may be found from coherent patterns of oscillations. Computationally, this can be done measuring the "period" of such oscillating patterns, or applying strict filtering so that each pattern becomes one oscillation, and then compute the tbp.

With the estimation of τ_w and a sufficiently large m, the reconstruction is completely defined and can be used for further analysis of the time series. Regarding the correlation dimension, an initial estimate may be derived with $\tau_w = \tau_p$, and then checking whether the same estimate is obtained when τ_w is increased. For noisy data, the estimate remains the same only for τ_w close to τ_p, as noise sets an upper limit to τ_w. The proposed parameter setting turned out to give the most confident ν-estimates for all data analyzed where estimation was possible.

16
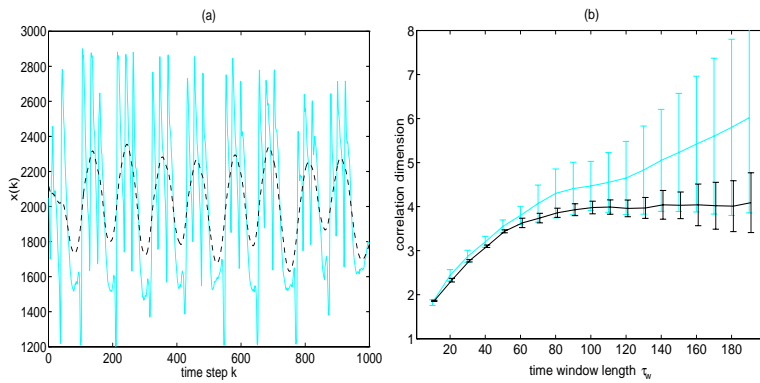
Figure 13: (a) Segment of the EEG time series of an epileptic seizure sampled with $\tau_s = 0.005 sec$ (solid grey line) and after smoothing with a 40 point FIR filter (stippled black line). (b) Plot of the correlation dimension estimate ν for MOD reconstruction with different τ_w for EEG time series in epileptic seizure. The grey curve with grey error bars correspond to estimation over a scaling interval $[r_1, r_2]$ with $r_2/r_1 = 4$ while the black curve with black error bars correspond to $r_2/r_1 = 2$. The other parameters are $N = 3400$, $\tau_s = 0.005$ and $\rho = 10$.

Acknowledgements

17

References

[1] D. Kugiumtzis, B. Lillekjendlie, and N. Christophersen. Chaotic time series part I: Estimation of some invariant properties in state space. *Modeling, Identification and Control*, 15(4):205 – 224, 1994.

[2] B. Lillekjendlie, D. Kugiumtzis, and N. Christophersen. Chaotic time series part II: System identification and prediction. *Modeling, Identification and Control*, 15(4):225 – 243, 1994.

[3] N. H. Packard, J. P. Crutchfield, J. D. Farmer, and R. S. Shaw. Geometry from a time series. *Physical Review Letters*, 45:712, 1980.

[4] F. Takens. Detecting strange attractors in turbulence. In D. A. Rand and L. S. Young, editors, *Dynamical Systems and Turbulence, Warwick 1980*, Lecture Notes in Mathematics 898, pages 366 – 381. Springer, Berlin, 1981.

[5] R. Mañé. On the dimensions of the compact invariant sets of certain non-linear maps. In D. A. Rand and L. S. Young, editors, *Dynamical Systems and Turbulence, Warwick 1980*, Lecture Notes in Mathematics 898, pages 230 – 242. Springer, Berlin, 1981.

[6] T. Sauer, J. A. Yorke, and M. Casdagli. Embedology. *Journal of Statistical Physics*, 65:579 – 616, 1991.

[7] D. S. Broomhead and G. P. King. Extracting qualitative dynamics from experimental data. *Physica D*, 20:217 – 236, 1986.

[8] J. G. Caputo, B. Malraison, and P. Atten. Determination of attractor dimension and entropy for various flows: An experimentalist's viewpoint. In G. Mayer-Kress, editor, *Dimensions and Entropies in Chaotic Systems*, pages 180 – 190. Springer-Verlag, Berlin, 1986.

[9] A. M. Albano, J. Muench, C. Schwartz, A. I. Mees, and P. E. Rapp. Singular value decomposition and the Grassberger-Procaccia algorithm. *Physical Review A*, 38(6):3017 – 3026, 1988.

[10] P. Grassberger, T. Schreiber, and C. Schaffrath. Non-linear time sequence analysis. *International Journal of Bifurcation and Chaos*, 1:521 – 547, 1991.

[11] J. F. Gibson, J. D. Farmer, M. Casdagli, and S. Eubank. An analytic approach to practical state space reconstruction. *Physica D*, 57:1 – 30, 1992.

[12] M. T. Rosenstein, J. J. Collins, and C. J. De Luca. Reconstruction expansion as a geometry-based framework for choosing proper delay times. *Physica D*, 73:82 – 98, 1994.

[13] P. Grassberger and I. Procaccia. Measuring the strangeness of strange attractors. *Physica D*, 9:189 – 208, 1983.

[14] T. Buzug and G. Pfister. Comparison of algorithms calculating optimal embedding parameters for delay time coordinates. *Physica D*, 58:127 – 137, 1992.

[15] G. Kember and A. C. Fowler. A correlation function for choosing time delays in phase portrait reconstructions. *Physics Letters A*, 179:72 – 80, 1993.

[16] E. N. Lorenz. Deterministic nonperiodic flow. *J. Atmos. Sci.*, 20:130, 1963.

[17] A. A. Tsonis. *Chaos: From Theory to Applications*. Plenum Press, New York, 1992.

[18] A. M. Fraser and H. Swinney. Independent coordinates for strange attractors from mutual information. *Physical Review A*, 33:1134 – 1140, 1986.

[19] A. Brandstater and H. Swinney. Strange attractors in weakly turbulent Couette-Taylor flow. *Physical Review A*, 35:2207 – 2220, 1987.

[20] M. B. Kennel, R. Brown, and H. D. I. Abarbanel. Determining embedding dimension for phase-space reconstruction using a geometrical construction. *Physical Review A*, 45:3403 – 3411, 1992.

[21] M. B. Kennel and H. D. I. Abarbanel. False neighbors and false strands: A reliable minimum embedding dimension algorithm. *Preprint*, 1995.

[22] W. Liebert, K. Pawelzik, and H. G. Schuster. Optimal embeddings of chaotic attractors from topological considerations. *Europhysics Letters*, 14(6):521 – 526, 1991.

[23] Z. Aleksić. Estimating the embedding dimension. *Physica D*, 52:362 – 368, 1991.

[24] H. D. I. Abarbanel, R. Brown, J. J. Sidorowich, and L. S. Tsimring. Analysis of observed chaotic data in physical systems. *Reviews of Modern Physics*, 65(4):1331 – 1392, 1993.

[25] R. Vautard, P. Yiou, and M. Ghil. Singular-spectrum analysis: A toolkit for short, noisy chaotic signals. *Physica D*, 58:95 – 126, 1992.

[26] A. I. Mees, P. E. Rapp, and L. S. Jennings. Singular-value decomposition and embedding dimension. *Physical Review A*, 36(1):340 – 346, 1987.

[27] A. Passamante, T. Hediger, and M. Gollub. Fractal dimension and local intrinsic dimension. *Physical Review A*, 39(7):3640 – 3645, 1989.

[28] A. Medio. *Chaotic Dynamics: Theory and Applications to Economics*. Cambridge University Press, Cambridge, 1992.

[29] E. Ott. *Chaos in Dynamical Systems*. Cambridge University Press, Cambridge, 1993.

[30] L. F. Olsen and H. Degn. Chaos in biological systems. *Guarterly Reviews of Biophysics*, 18:165 – 225, 1985.

[31] M. I. Rabinovich and A. L. Fabrikant. Stochastic self-modulation of waves in nonequilibrium media. *Sov. Phys. JETP*, 50:311, 1979.

[32] M. Mackey and L. Glass. Oscillation and chaos in physological control systems. *Science*, 197:287, 1977.

[33] M. Ding, C. Grebogi, E. Ott, T. Sauer, and J. A. Yorke. Estimating correlation dimension from a chaotic time series: when does a plateau onset occur? *Physica D*, 69:404 – 424, 1993.

[34] O. E. Rössler. An equation for continuous chaos. *Physics Letters A*, 57:397 – 398, 1976.

[35] A. M. Albano, A. Passamante, and M-E. Farell. Using higher-order correlations to define an embedding window. *Physica D*, 54:85 – 97, 1991.

[36] J. M. Martinerie, A. M. Albano, I. A. Mees, and P. E. Rapp. Mutual information, strange attractors, and the optimal estimation of dimension. *Physical Review A*, 45(10):7058 – 7064, 1992.

[37] D Kugiumtzis. Assessing different norms in nonlinear analysis of noisy time series. *Preprint*, 1996.

[38] J. Theiler. Estimating fractal dimension. *J. Opt. Soc. Am. A*, 7(6):1055 – 071, 1990.

[39] O. E. Rössler. An equation for hyperchaos. *Physics Letters A*, 71(2 – 3):155 – 157, 1979.

[40] B. H. Jansen. Quantitative analysis of electroencephalograms: is there chaos in the future? *International Journal of Biomedical Computing*, 27:95 – 123, 1991.

[41] H. Kantz and T. Schreiber. Dimension estimates and physiological data. *Chaos*, 5(1):143 – 154, 1995.

[42] P. E. Rapp, I. D. Zimmerman, A. M. Albano, G. C. Deguzman, and N. N. Greenbaum. Dynamics of spontaneous neural activity in the simian motor cortex: the dimension of chaotic neurons. *Physics Letters A*, 110:335 – 338, 1985.

[43] A. Babloyantz and A. Destexhe. Low-dimensional chaos in an instance of epilepsy. *Proceedings of the National Academy of Sciences of the United States of America*, 83:3513 – 3517, 1986.

[44] G. W. Frank, T. Lookman, M. A. H. Nerenberg, C. Essex, J. Lemieux, and W Blume. Chaotic time series analyses of epileptic seizures. *Physica D*, 46:427 – 438, 1990.

[45] J. P. Pijn, J. V. Neerven, A. Noest, and F. H. Lopes da Silva. Chaos or noise in EEG signals; dependence on state and brain site. *Electroencephalography and Clinical Neurophysiology*, 79:371 – 381, 1991.

[46] D. W. Pritchard and W. S. Duke. Measuring chaos in the brain: A tutorial review of nonlinear dynamical EEG analysis. *Intern J. Neuroscience*, 67:31 – 80, 1992.

[47] H Madsen. Non-linear methods for the analysis of electroencephalograms (EEG). Master's thesis, Department of Informatics, Oslo, 1995. 186 pp (in Norwegian).